Highly anisotropic energy gap in superconducting $Ba(Fe_{0.9}Co_{0.1})_2As_2$ from optical conductivity measurements

T. Fischer, A. V. Pronin,* and J. Wosnitza
Dresden High Magnetic Field Laboratory (HLD), FZ Dresden-Rossendorf, 01314 Dresden, Germany

K. Iida, F. Kurth, S. Haindl, L. Schultz, and B. Holzapfel
IFW Dresden, Institute for Metallic Materials, 01171 Dresden, Germany

E. Schachinger
Institute of Theoretical and Computational Physics, Graz University of Technology, 8010 Graz, Austria

(Dated: September 23, 2010)

We have measured the complex dynamical conductivity, $\sigma = \sigma_1 + i\sigma_2$, of superconducting $Ba(Fe_{0.9}Co_{0.1})_2As_2$ ($T_c = 22$ K) at terahertz frequencies and temperatures 2 - 30 K. In the frequency dependence of σ_1 below T_c, we observe clear signatures of the superconducting energy gap opening. The temperature dependence of σ_1 demonstrates a pronounced coherence peak at frequencies below 15 cm^{-1} (1.8 meV). The temperature dependence of the penetration depth, calculated from σ_2, shows power-law behavior at the lowest temperatures. Analysis of the conductivity data with a two-gap model, gives the smaller isotropic s-wave gap of $\Delta_A = 3$ meV, while the larger gap is highly anisotropic with possible nodes and its rms amplitude is $\Delta_0 = 8$ meV. Overall, our results are consistent with a two-band superconductor with an $s_\pm$ gap symmetry.

PACS numbers: 74.25.Gz, 74.25.nd, 74.70.Xa

I. INTRODUCTION

The issue of the symmetry of the superconducting order parameter in the iron-pnictide superconductors remains unsettled. Shortly after the discovery of superconductivity in these materials[1] models, which predict the order parameter to change its sign on different sheets of the Fermi surface (FS), have been put forward.[2,3] In the simplest case of the $s_\pm$-wave symmetry, the superconducting gap Δ can be parameterized as $\Delta = \Delta_0/2 \cdot (\cos k_x + \cos k_y)$. Because the FS of the pnictides consists of two distinct set of sheets, centered at the Γ (hole pocket) and M (electron pocket) points of the Brillouin zone, there are no nodes in this gap.

Many experiments, including e.g. ARPES, are indeed consistent with this picture.[4–8] There is, however, a large body of experimental works, which cannot be easily explained assuming the nodeless gap scenario.[9–12] Possibly, the gap function of the iron pnictides is not universal – whether the gap is nodeless or not might depend on the compound and on the doping level. In order to account for this non-universal behavior, models with relatively large intraband Coulomb repulsion within the FS pockets have been proposed, resulting in gap symmetries varying between extended s-wave $[\cos(k_x)\cos(k_y)]$, d_{xy} wave, and $d_{x^2-y^2}$ wave, all allowing for nodes in the order parameter.[13–16]

Currently, the so-called 122 iron-pnictide family (doped AFe_2As_2, A = Ba, Sr, Ca) seems to be best suited for experimental investigations due to the availability of relatively large single crystals as well as thin epitaxial films of high quality.[18–22] In this article we focus on $Ba(Fe_{1-x}Co_x)_2As_2$. Thermal conductivity measurements, performed at temperatures down to 50 mK, indicate a nodeless in-plane gap in this compound.[23,24] The gap is reported to remain nodeless at all doping levels – from under- to overdoped, but the gap anisotropy increases with doping. This is consistent with APRES results, which systematically show a full gap in all pnictide compounds.[5,6,25,26]

Optical spectra of superconductors contain information about the size and the symmetry of the superconducting gaps. Since the last two years, a large number of reports on optical properties of pnictides has been published (see Ref. 17 for a review). The low-frequency (terahertz-far-infrared) optical properties of the electron-doped 122 pnictides have recently been investigated by a few groups for doping levels near optimal.[27–33] There is, however, neither consensus in these reports about the gap sizes, nor about the number of gaps (although the majority of reports agrees on a two-gap picture). Obviously, the analysis of the optical spectra is challenged by the fact, that the gaps are likely to be different on different sheets of the FS.

Our method allows us to perform not only frequency-dependent measurements, but also measurements of the optical parameters as a function of temperature at fixed frequencies. This gives advantages over standard optical studies, since frequency and temperature dependences of optical parameters can be analyzed simultaneously.

Here, we report on the observation of clear signatures of the superconducting-gap opening in the terahertz optical conductivity. Through the temperature-dependent measurements and theoretical analysis, we show the gap

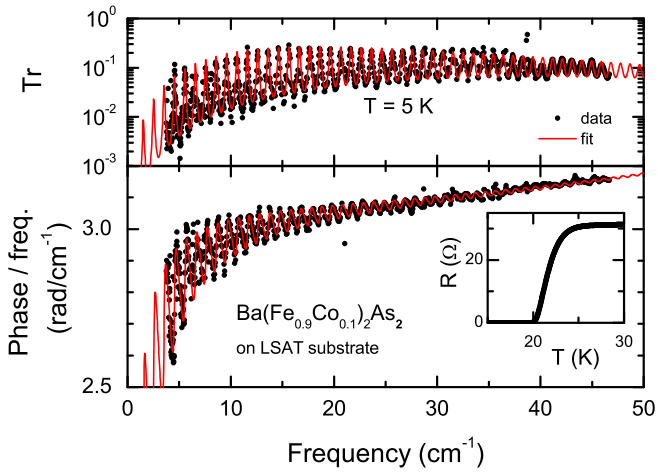

FIG. 1: (Color online) Examples of as-measured spectra of the transmission coefficient (upper frame) and the phase shift of the transmitted wave (bottom frame) for a 20 nm $Ba(Fe_{0.9}Co_{0.1})_2As_2$ film on a (La,Sr)(Al,Ta)O_3 substrate at $T = 5$ K. The solid lines represent fit using a two-fluid model. The phase shift spectra are divided by frequency for better representation. Inset: resistance of the film around the superconducting transition.

is highly anisotropic with possible nodes on at least one sheet of the FS.

II. EXPERIMENT

Films of $Ba(Fe_{0.9}Co_{0.1})_2As_2$ have been grown by pulsed laser deposition on (001)-orientated $(La_{0.7}Sr_{0.3})(Al_{0.65}Ta_{0.35})O_3$ (LSAT) substrates, transparent for terahertz radiation. The $Ba(Fe_{0.9}Co_{0.1})_2As_2$ target was ablated with 248 nm KrF radiation under UHV conditions.[21] The phase purity was confirmed by x-ray diffraction in Bragg-Brentano geometry. The c axes of the films was normal to the film surface. The thickness of the films, used for the measurements, was measured by ellipsometry. Standard four-probe method has been used to measure the dc resistivity. We have investigated two $Ba(Fe_{0.9}Co_{0.1})_2As_2$ films with thicknesses of 20 and 100 nm. The results of our investigations for both films are qualitatively the same. However, the optical transmissivity of the thinner film is obviously higher, leading to a much better signal-to-noise ratio. That is why in this paper we present results for the thinner film only. The resistive onset of the superconducting transition in the film appeared at 25 K (Fig. 1, inset). The substrate was a plane-parallel plate, approximately 10×10 mm in size with thickness of 1.025 mm.

In the frequency range 4 - 47 cm^{-1} (120 - 1400 GHz, 0.5 - 5.8 meV) the measurements have been performed with a spectrometer, which uses backward-wave oscillators (BWOs) as sources of coherent and frequency-tunable radiation.[34] A Mach-Zehnder interferometer arrangement of the spectrometer allows to measure both the intensity and the phase shift of the wave transmitted through the $Ba(Fe_{0.9}Co_{0.1})_2As_2$ film and the substrate[35]. Using the Fresnel optical formulas for the complex transmission coefficient of the two-layer system, both components of the complex conductivity $(\sigma_1 + i\sigma_2)$ of the film have been calculated. The optical parameters of the substrate have been found by measuring a bare substrate without film. This experimental method has been previously applied to a large number of different superconductors.[36] In addition to the "standard" frequency sweeps at fixed temperatures, we performed temperature sweeps at fixed frequencies in the same way as it has been done e.g. in Ref. 37. This allows for a more thorough monitoring of the temperature dependence of σ_1 and σ_2.

III. RESULTS

Figure 1 shows as-measured transmission $Tr(\nu)$ and phase-shift $\varphi(\nu)$ spectra as a function of frequency, $\nu = \omega/2\pi$. The measurements are done with a number of different BWOs covering the range from 4 to 47 cm^{-1} continuously. Since the major term of the phase shift is proportional to the frequency of the probing radiation, the phase-shift spectra are divided by frequency to eliminate the constant frequency slope. The pronounced fringes in both $Tr(\nu)$ and $\varphi(\nu)$ are due to the multiple interference inside the substrate, which acts as a Fabry-Perot interferometer. As the complete Fresnel formulas for a two-layer system are used, these fringes are automatically taken into account in the calculations of the complex conductivity.

Figure 2 shows spectra of the real (upper frame) and imaginary (bottom frame) part of the complex conductivity of $Ba(Fe_{0.9}Co_{0.1})_2As_2$ at selected temperatures above and below T_c.

The normal-state complex conductivity demonstrates typical Drude behavior, $\sigma(\omega) = \sigma_{dc}/(1 - i\omega\tau)$. From simultaneous fit of $\sigma_1(\omega)$ and $\sigma_2(\omega)$ at 30 K (dashed line in Fig. 2), we find $\sigma_{dc} = 6000\ \Omega^{-1}$cm^{-1} and the scattering rate $\gamma = 1/2\pi\tau = 200$ cm^{-1} ($\tau = 2.7 \times 10^{-14}$ s), the former is in agreement with our dc measurements, and the later coincides with the scattering rate, obtained via $\gamma = \sigma_1(\omega)\omega/\sigma_2(\omega)$ from the complex conductivity spectra (γ obtained in this way has, however, a larger error bar due to the large scattering of data points in σ_2). From $(\omega_p/2\pi)^2 = 2\sigma_{dc}\gamma$, we estimate the plasma frequency of the Drude component in the normal state, $\omega_p/2\pi = 8500$ cm^{-1} (1.05 eV).

When entering the superconducting state the energy gap opens, as reflected in the lowering of σ_1 below T_c (upper frame of Fig. 2). For an isotropic s-wave superconductor at $T = 0$ a sharp frequency onset of $\sigma_1(\omega)$ is expected at $2\Delta(0)$. The absence of such a feature in our frequency window implies that the energy gap $\Delta(0)$ (or

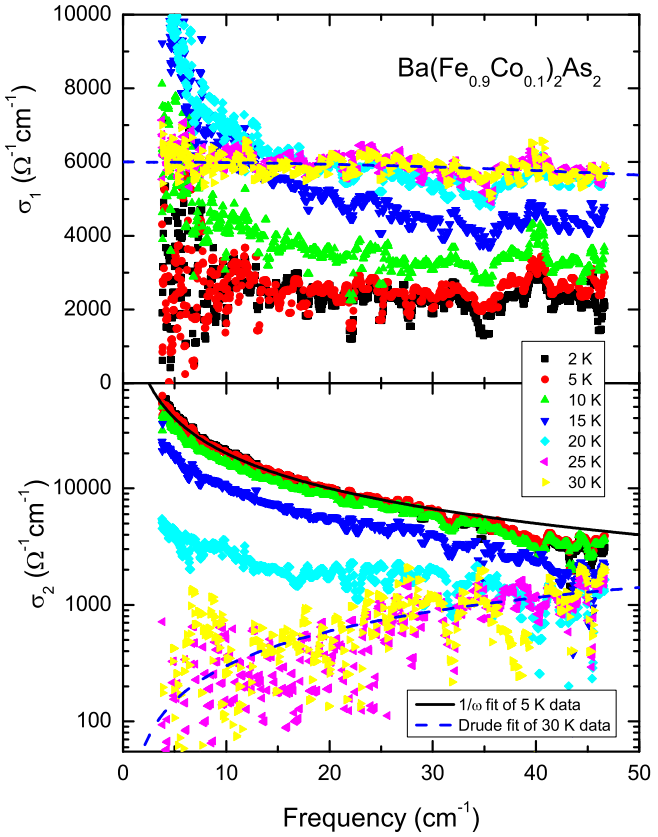

FIG. 2: (Color online) Frequency dependence of the real, σ_1, (upper panel) and the imaginary, σ_2, (bottom panel) parts of the complex conductivity of $Ba(Fe_{0.9}Co_{0.1})_2As_2$ for selected temperatures above and below T_c. The solid line is a fit of the 5 K σ_2 data with $\sigma_2 \propto 1/\omega$. The dashed line is a fit of the 30 K data with a Drude term. Note the logarithmic Y-scale of the bottom panel.

one of the gaps for a multi-band superconductor) must be larger than $47/2 = 23.5$ cm^{-1} (2.9 meV). This result is consistent with the majority of optical measurements in $Ba(Fe_{1-x}Co_x)_2As_2$ – the 2Δ feature is usually seen at 50 cm^{-1} or somewhat higher frequency.[27,28,32,33]

The appearance of a δ-function at $\omega = 0$ in $\sigma_1(\omega)$ below T_c leads (*via* the Kramers-Kronig relation) to an $1/\omega$-divergence in $\sigma_2(\omega)$, clearly visible in the bottom frame of Fig. 2 for $T \leq 20$ K. The strength of this divergence (the pre-factor) is a direct measure of the weight of the superconducting condensate. From the $\sigma_2(\omega)$ data, one can directly extract the penetration depth *via*

$$\lambda = c/(4\pi\sigma_2\omega)^{1/2}. \quad (1)$$

At 2 K, we find $\lambda = 0.45 \pm 0.02$ μm, which gives for the plasma frequency of the superconducting condensate, $\omega_{ps} = c/\lambda$, the value of 3600 cm^{-1} (450 meV), corresponding to the spectral weight of $(\omega_{ps}/2\pi)^2 = (1.3 \pm 0.1) \times 10^7$ cm^{-2}. These values are within the margins set by previous reports on terahertz measurements of $Ba(Fe_{1-x}Co_x)_2As_2$ films.[29,38]

For low enough frequencies and temperatures, where normal carriers are not affecting σ_2, an analysis of the temperature-dependent penetration depth is meaningful. We have extracted λ as a function of temperature for a number of frequencies (Fig. 3). For $T < 0.2T_c$, we observe a clear power law behavior. As can be seen from this figure, the power law has an exponent slightly higher than 2, which is in agreements with microwave measurements.[39,40]

IV. ANALYSIS AND DISCUSSION

Let us now turn to the analysis of the conductivity data. As it can be seen from the upper panel of Fig. 2, at frequencies below 15 cm^{-1}, the temperature dependence of σ_1 below T_c is non-monotonic. Upon entering the superconducting state, σ_1 first rises, and then drops. In order to monitor this temperature dependence in more detail, we performed temperature sweeps at fixed frequencies (Fig. 4). At low frequencies, a prominent coherence peak appears in σ_1. Multi-gap effects and gap symmetry are known to have crucial influence on the coherence peak appearance.[41,42]

The analysis of the data is performed in the spirit of Ref. 42. We use an $s + d$-wave gap[43] as a model for the extended s-wave, which is one part of the $s_\pm$ model. We can do this because optics cannot resolve the phase difference, thus for the optics the $s_\pm$ model just consist of one isotropic s-wave gap (Δ_A, hole pocket) and a second extended s-wave gap, which, in our case, is modeled using an $s + d$-wave symmetric gap when referred to the M-

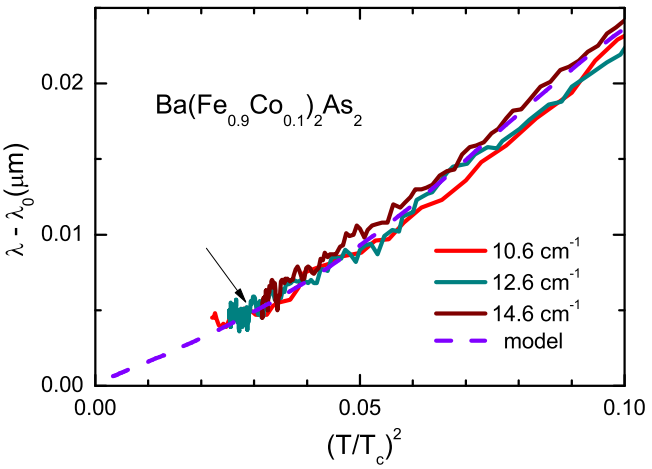

FIG. 3: (Color online) Temperature variation of the penetration depth of $Ba(Fe_{0.9}Co_{0.1})_2As_2$ as a function of T^2. The solid lines are experimental data. The error bars are set by the scatting of the data points. The dashed line is $\lambda(\omega = 0)$ obtained with the two-gap model discussed in the text. The arrow indicates the point where the theoretical line has been normalized to the experimental value ($(T/T_c)^2 = 0.03$). The mid-point of the transition (22 K) has been taken as T_c.

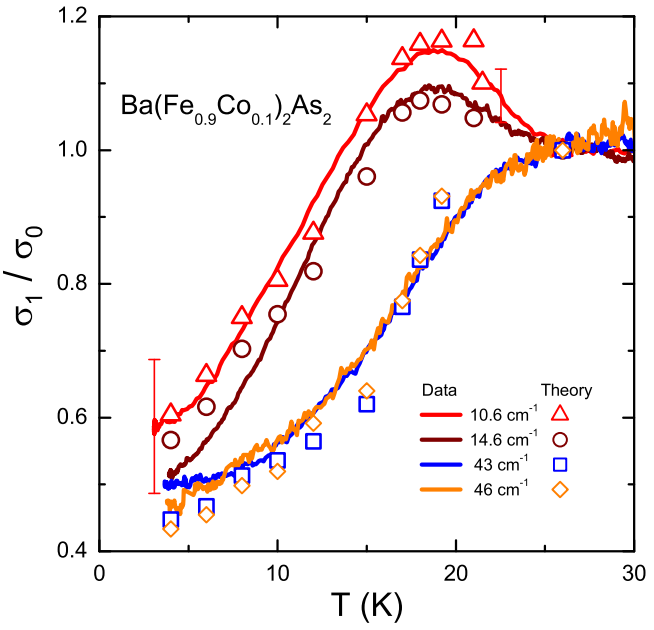

FIG. 4: (Color online) Temperature dependence of the real part of the complex conductivity in $Ba(Fe_{0.9}Co_{0.1})_2As_2$. The values are normalized to the respective normal-state conductivity at $T = 26$ K (σ_0). Lines - experiment, dots - calculations with the two-gap model discussed in the text.

point. This model is also described in greater detail in Ref. 44.

The gap on the electron pocket is parameterized as $\Delta_B = \Delta_s + \Delta_d\sqrt{2}\cos(2\theta)$ (here Δ_s is the s-wave component, Δ_d is the amplitude of the d-wave component, and θ is the polar angle on the FS). An anisotropy parameter α has been introduced in such a way that $\Delta_s = \alpha\Delta_0$, $\Delta_d = \sqrt{1-\alpha^2}\Delta_0$, and $\Delta_0 = \sqrt{\langle\Delta_B^2(\theta)\rangle_\theta}$ ($\langle...\rangle_\theta$ is the FS average). In the clean limit, this gap has nodes, if $\alpha \leq \sqrt{2/3}$.

For convenience, one can introduce the parameter $X = \alpha/(\alpha + \sqrt{1-\alpha^2}) \times 100\%$, which gives the percentage of the s-wave component in the $s+d$-wave admixture. The temperature dependence of the superconducting gaps has been modeled by the standard mean-field BCS temperature dependence with $T_c = 22$ K (the midpoint of the transition). The complex conductivity is a sum of two weighted components, corresponding to the two FS pockets: $\sigma(\omega,T) = w_1\sigma^{(1)}(\omega,T) + w_2\sigma^{(2)}(\omega,T)$, and $w_1 + w_2 = 1$.

In our analysis we concentrated on the 10.6 cm^{-1} data set following the procedure outlined by Schachinger and Carbotte.[42] The size of the two gaps, the s-wave contribution (X) to the anisotropic gap, and the weights w_1 and w_2 were adjusted in order to reproduce the temperature dependence of the normalized conductivity σ_1/σ_0 as good as possible. We obtained the best fit with $\Delta_A = 3$ meV $= 24$ cm^{-1}, $\Delta_0 = 8$ meV $= 64$ cm^{-1}, and $X = 33.5\%$, corresponding to $\alpha = 0.45$ and indicating the existence of nodes. The weights of the FS pockets were found to be $w_1 = 20\%$ for the hole and $w_2 = 80\%$ for the electron pocket, the normal-state elastic scattering rate being equal to 22 meV (180 cm^{-1}).[45]

The model calculations for the other three frequencies (14.6, 43, and 46 cm^{-1}) are found to follow the experimental data without any further adjustment of the primary parameters. The theory predicts, assuming an instantaneous transition, that the 43 and 46 cm^{-1} data sets should also show a coherence peak at $T \approx 21.5$ K. This temperature, however, is already well within the superconducting transition of the film and thus, such peaks cannot be observed experimentally. What is left as a very convincing result is the correct reproduction of the coherence peak for 10.6 and 14.6 cm^{-1} and a very good agreement with the data measured at 43 and 46 cm^{-1} for $T \leq 20$ K.

We calculated, moreover, using the model discussed previously the low temperature variation of the penetration depth in the zero frequency limit.[46] The result is presented in Fig. 3 as the dashed line. At $(T/T_c)^2 < 0.1$, the agreement between the model and the experimental data is perfect.[47]

Another explanation for the low-temperature T^2 dependence of the penetration depth was given by Vorontsov *et al.*[48] These authors studied the superconducting $s_\pm$ symmetry state and concluded that the strong interband interaction (scattering) is strongly pair-breaking and that the superconductor is driven into a gapless state. For this state the authors prove that the penetration depth will be $\propto T^2$ at low temperatures. A similar result was reported by Gordon *et al.*[49] who studied a highly anisotropic single s-wave superconductor with a high concentration of pair-breaking impurities which will also drive the superconductor into a gapless state. They argued that because of the assumed high anisotropy this model must not necessarily be in contradiction to the thermal conductivity results of Tanatar *et al.*[23]

Authors of recent optical measurements of $Ba(Fe_{1-x}Co_x)_2As_2$ argue for interpretation of the conductivity data in terms of an $s_\pm$ state with strong pair-breaking scattering.[33,50] Nevertheless, it is necessary to point out that Nicol and Carbotte[51] studied the optical properties of a classical s-wave superconductor with magnetic impurities. They come to the conclusion that in the gapless state (strong pair-braking) a coherence peak becomes strongly suppressed which is in clear contradiction to our results presented in Fig. 4. Likely, as it has been proposed in Ref. 33, both effects, the large gap anisotropy and the pair-braking scattering have to be taken into account in order to describe the optical conductivity in the pnictides. No detailed model for such a calculation has been developed yet. The analysis performed in Ref. 33, however, suggests that only a minor part of σ_1 in the superconducting state below the gap can be due to the pair-breaking effects, while the major contribution is due to the nodes or at least strong gap anisotropy.

Our observation of a superconducting gap with nodes is, at a first glance, at odds with the results of Tanatar *et al.*[23] However, the s+d-wave model used by us to describe the anisotropic superconducting gap around the M-point of the Brillouin zone provides a mechanism called "lifting of the nodes", first discussed by Mishra *et al.*[52] and later on studied explicitly in Ref. 44. The model allows a lifting of the nodes in the superconducting gap given a high enough s-wave contribution to the $s+d$-wave admixture and additional elastic scattering. This mechanism is also temperature dependent and it is more likely to lift existing nodes the lower the temperature. Thus, it is possible within this model that at very low temperatures, like the ones used by Tanatar *et al.*,[23] a small spectral gap can develop in the real part of the optical conductivity. Increasing the temperature will smear out this small gap and σ_1 will show nodal behavior at higher temperatures. Most recent thermal conductivity measurements give evidence of a small gap (almost nodes) in regions of the FS which contribute significantly to in-plane conduction.[24]

V. CONCLUSIONS

We found the superconducting energy gap in $Ba(Fe_{0.9}Co_{0.1})_2As_2$ to be highly anisotropic. This anisotropy is responsible for the broad and pronounced coherence peak observed in σ_1 which is in clear contradiction to a gapless superconducting state. A two-gap model – isotropic s-wave gap for the hole pocket and an $s+d$-wave gap for the electron pocket of the FS (Ref. 42) – has been applied to mimic the $s_\pm$ gap symmetry. The model provides a very good description of the $\sigma_1(T)$ curves measured at different frequencies. In the framework of this model, we have found the value of 3 meV for the isotropic gap and an rms amplitude of 8 meV for the second gap which is also found to be nodal. It was possible using this model to reproduce consistently not only the energy and temperature dependence of σ_1 in the terahertz region but also the low temperature variation of the penetration depth.

VI. ACKNOWLEDGEMENTS

We would like to thank Jules P. Carbotte and Ilya Eremin for useful discussions and Mykola Vinnichenko for the film-thickness measurements. Part of this work was supported by EuroMagNET II (EU contract No. 228043).

* Electronic address: a.pronin@fzd.de

1. Y. Kamihara, T. Watanabe, M. Hirano, and H. Hosono, J. Am. Chem. Soc. **130**, 3296 (2008).
2. I. I. Mazin, D. J. Singh, M. D. Johannes, and M. H. Du, Phys. Rev. Lett. **101**, 057003 (2008).
3. K. Kuroki, S. Onari, R. Arita, H. Usui, Y. Tanaka, H. Kontani, and H. Aoki, Phys. Rev. Lett. **101**, 087004 (2008).
4. A. D. Christianson, E. A. Goremychkin, R. Osborn, S. Rosenkranz, M. D. Lumsden, C. D. Malliakas, I. S. Todorov, H. Claus, D. Y. Chung, M. G. Kanatzidis, R. I. Bewley, and T. Guidi, Nature **456**, 930 (2008).
5. D. V. Evtushinsky, D. S. Inosov, V. B. Zabolotnyy, A. Koitzsch, M. Knupfer, B. Büchner, M. S. Viazovska, G. L. Sun, V. Hinkov, A. V. Boris, C. T. Lin, B. Keimer, A. Varykhalov, A. A. Kordyuk, and S. V. Borisenko, Phys. Rev. B **79**, 054517 (2009).
6. K. Terashima, Y. Sekiba, J. H. Bowen, K. Nakayama, T. Kawahara, T. Sato, P. Richard, Y.-M. Xu, L. J. Li, G. H. Cao, Z.-A. Xu, H. Ding, and T. Takahashi, Proc. Natl. Acad. Sci. **106**, 7330 (2009).
7. T. J. Williams, A. A. Aczel, E. Baggio-Saitovitch, S. L. Budko, P. C. Canfield, J. P. Carlo, T. Goko, J. Munevar, N. Ni, Y. J. Uemura, W. Yu, and G. M. Luke, Phys. Rev. B **80**, 094501 (2009).
8. F. Hardy, T. Wolf, R. A. Fisher, R. Eder, P. Schweiss, P. Adelmann, H. v. Loehneysen, C. Meingast, Phys. Rev. B **81**, 060501(R) (2010).
9. C. Martin, R. T. Gordon, M. A. Tanatar, H. Kim, N. Ni, S. L. Budko, P. C. Canfield, H. Luo, H. H. Wen, Z. Wang, A. B. Vorontsov, V. G. Kogan, and R. Prozorov, Phys. Rev. B **80**, 020501(R) (2009).
10. B. Muschler, W. Prestel, R. Hackl, T. P. Devereaux, J. G. Analytis, J.-H. Chu, and I. R. Fisher, Phys. Rev. B **80**, 180510(R) (2009).
11. S. Salem-Sugui, L. Ghivelder, A. D. Alvarenga, J. L. Pimentel, H. Luo, Zh. Wang, and H.-H. Wen, Phys. Rev. B **80**, 014518 (2009).
12. T. Goko, A. A. Aczel, E. Baggio-Saitovitch, S. L. Budko, P. C. Canfield, J. P. Carlo, G. F. Chen, P. Dai, A. C. Hamann, W. Z. Hu, H. Kageyama, G. M. Luke, J. L. Luo, B. Nachumi, N. Ni, D. Reznik, D. R. Sanchez-Candela, A. T. Savici, K. J. Sikes, N. L. Wang, C. R. Wiebe, T. J. Williams, T. Yamamoto, W. Yu, and Y. J. Uemura, Phys. Rev. B **80**, 024508 (2009).
13. A. V. Chubukov, M. G. Vavilov, and A. B. Vorontsov, Phys. Rev. B **80**, 140515 (2009).
14. A. Moreo, M. Daghofer, J. A. Riera, and E. Dagotto, Phys. Rev. B **79**, 134502 (2009).
15. T. A. Maier, S. Graser, D. J. Scalapino, and P. J. Hirschfeld, Phys. Rev. B **79**, 224510 (2009).
16. K. Kuroki, H. Usui, S. Onari, R. Arita, and H. Aoki, Phys. Rev. B **79**, 224511 (2009).
17. W. Z. Hu, Q. M. Zhang, and N. L. Wang, Physica C **469**, 545 (2009).
18. A. S. Sefat, R. Jin, M. A. McGuire, B. C. Sales, D. J. Singh, and D. Mandrus, Phys. Rev. Lett. **101**, 117004 (2008).
19. H. Hiramatsu, T. Katase, T. Kamiya, M. Hirano, and H. Hosono, Appl. Phys. Express **1**, 101702 (2008).
20. T. Katase, H. Hiramatsu, H. Yanagi, T. Kamiya, M. Hirano, and H. Hosono, Solid State Commun. **149**, 2121 (2009).
21. K. Iida, J. Hänisch, R. Hühne, F. Kurth, M. Kidszun, S.

Haindl, J. Werner, L. Schultz, and B. Holzapfel, Appl. Phys. Lett. **95**, 192501 (2009).

[22] S. Lee, J. Jiang, Y. Zhang, C. W. Bark, J. D. Weiss, C. Tarantini, C. T. Nelson, H. W. Jang, C. M. Folkman, S. H. Baek, A. Polyanskii, D. Abraimov, A. Yamamoto, J. W. Park, X. Q. Pan, E. E. Hellstrom, D. C. Larbalestier, and C. B. Eom, Nat. Mater. **9**, 397 (2010).

[23] M. A. Tanatar, J.-Ph. Reid, H. Shakeripour, X. G. Luo, N. Doiron-Leyraud, N. Ni, S. L. Budko, P. C. Canfield, R. Prozorov, and L. Taillefer, Phys. Rev. Lett. **104**, 067002 (2010).

[24] J.-Ph. Reid, M. A. Tanatar, X. G. Luo, H. Shakeripour, N. Doiron-Leyraud, N. Ni, S. L. Bud'ko, P. C. Canfield, R. Prozorov, and L. Taillefer, Phys. Rev. B **82**, 064501 (2010).

[25] T. Kondo, A. F. Santander-Syro, O. Copie, Chang Liu, M. E. Tillman, E. D. Mun, J. Schmalian, S. L. Budko, M. A. Tanatar, P. C. Canfield, and A. Kaminski, Phys. Rev. Lett. **101**, 147003 (2008)

[26] D. Qian, Y. Xia, L. Wray, D. Hsieh, M. Z. Hasan, J. Supercond. Nov. Magn. **23** 617 (2010).

[27] E. van Heumen, Y. Huang, S. de Jong, A. B. Kuzmenko, M. S. Golden, and D. van der Marel, Europhys. Lett. **90** 37005 (2010).

[28] K. W. Kim, M. Rössle, A. Dubroka, V. K. Malik, T. Wolf and C. Bernhard, Phys. Rev. B **81**, 214508 (2010).

[29] B. Gorshunov, D. Wu, A. A. Voronkov, P. Kallina, K. Iida, S. Haindl, F. Kurth, L. Schultz, B. Holzapfel, and M. Dressel, Phys. Rev. B **81**, 060509(R) (2010).

[30] D. Wu, N. Barišic, P. Kallina, A. Faridian, B. Gorshunov, N. Drichko, L. J. Li, X. Lin, G. H. Cao, Z. A. Xu, N. L. Wang, and M. Dressel, Phys. Rev. B **81**, 100512(R) (2010).

[31] A. Perucchi, L. Baldassarre, C. Marini, S. Lupi, J. Jiang, J. D. Weiss, E. E. Hellstrom, S. Lee, C. W. Bark, C. B. Eom, M. Putti, I. Pallecchi, and P. Dore, arXiv:1003.0565.

[32] M. Nakajima, S. Ishida, K. Kihou, Y. Tomioka, T. Ito, Y. Yoshida, C. H. Lee, H. Kito, A. Iyo, H. Eisaki, K. M. Kojima, and S. Uchida, Phys. Rev. B **81**, 104528 (2010).

[33] R. P. S. M. Lobo, Y. M. Dai, U. Nagel, T. Rõõm, J. P. Carbotte, T. Timusk, A. Forget, and D. Colson, arXiv:1007.3761.

[34] G. V. Kozlov and A. A. Volkov, in *Millimeter and Submillimeter Wave Spectroscopy of Solids*, edited by G. Grüner (Springer, Berlin, 1998), p. 51.

[35] B. Gorshunov, A. Volkov, I. Spektor, A. Prokhorov, A. Mukhin, M. Dressel, S. Uchida, and A. Loidl, Int. J. Infrared Millimeter Waves **26**, 1217 (2005).

[36] M. Dressel, N. Drichko, B. P. Gorshunov, and A. Pimenov, IEEE J. Sel. Top. Quantum Electron. **14**, 399 (2008) and references therein.

[37] A. V. Pronin, A. Pimenov, A. Loidl, A. Tsukada, and M. Naito, Phys. Rev. B **68**, 054511 (2003).

[38] D. Nakamura, Y. Imai, A. Maeda, T. Katase, H. Hiramatsu, and H. Hosono, arXiv:0912.4351.

[39] R. T. Gordon, N. Ni, C. Martin, M. A. Tanatar, M. D. Vannette, H. Kim, G. D. Samolyuk, J. Schmalian, S. Nandi, A. Kreyssig, A. I. Goldman, J. Q. Yan, S. L. Budko, P. C. Canfield, and R. Prozorov, Phys. Rev. Lett. **102**, 127004 (2009).

[40] R. Prozorov, M. A. Tanatar, R. T. Gordon, C. Martin, H. Kim, V. G. Kogan, N. Ni, M. E. Tillman, S. L. Budko, and P. C. Canfield, Physica C **469**, 582 (2009).

[41] O. V. Dolgov, A. A. Golubov, and D. Parker, New J. Phys. **11**, 075012 (2009).

[42] E. Schachinger and J. P. Carbotte, Phys. Rev. B **80**, 174526 (2009).

[43] I. Schürrer, E. Schachinger, and J. P. Carbotte, Physica C **303**, 287 (1998).

[44] J. P. Carbotte and E. Schachinger, Phys. Rev. B **81**, 104510 (2010).

[45] Analysis of far-infrared measurements of $Ba(Fe_{1-x}Co_x)_2As_2$ single crystal within the same two-band model gives very similar values for the paraments used. See, D. Wu, N. Barisic, M. Dressel, G. H. Cao, Z. A. Xu, J. P. Carbotte, E. Schachinger, arXiv:1007.5215.

[46] It has been demonstrated by R. Modre, I. Schürrer, and E. Schachinger, Phys. Rev. B **57**, 5496 (1998), that the $s + d$-wave model predicts low-temperature laws for the London penetration depth from linear (pure d-wave, $X = 0$) to exponential (pure s-wave, $X = 1$) depending on the amount of s-wave admixture (X) and the amount and type of elastic scattering in the system.

[47] Because our measurements are performed at relatively high frequencies, the contribution of the normal carriers to σ_2 (and, consequently, to λ, Eq. 1) becomes not negligible at higher temperatures, causing the experimetal data to deviate from the model curve calculated for $\omega = 0$.

[48] A. B. Vorontsov, M. G. Vavilov, and A. V. Chubukov, Phys. Rev. B **79**, 140507(R) (2009).

[49] R. T. Gordon, H. Kim, M. A. Tanatar, R. Prozorov, and V. G. Kogan, Phys. Rev. B **81**, 180501(R) (2010).

[50] R. Valdés Aguilar, L. S. Bilbro, S. Lee, J. Jiang, J. D. Weiss, E. E. Hellstrom, D. C. Larbalestier, C. B. Eom, N. P. Armitage, arXiv:1007.3677.

[51] E. J. Nicol and J. P. Carbotte, Phys. Rev. B **44**, 7741(R) (1991).

[52] V. Mishra, G. Boyd, S. Graser, T. Maier, P. J. Hirschfeld, and D. J. Scalapino, Phys. Rev. B **79**, 094512 (2009).